

# The Design and Evaluation of a Low Cost Haptic Device for Needle Puncture

M. R. Edwards<sup>1</sup> C. J. Hughes<sup>1</sup>, N. W. John<sup>1</sup>, S. Burnell<sup>2</sup>

<sup>1</sup>*School of Computer Science, Bangor University, UK.*

<sup>2</sup>*Consultant Anaesthetist, Ysbyty Gwynedd Hospital, Bangor. UK.*

*m.r.edwards@bangor.ac.uk, c.j.hughes@bangor.ac.uk, n.w.John@bangor.ac.uk*

## INTRODUCTION

Haptic devices are an essential component of many simulators for training medical procedures. For example, we previously demonstrated the importance of haptics in a Seldinger Technique simulator, which resists the needle as it punctures simulated vasculature [1, 2]. High cost of commercial haptic devices used for such simulations prompted our investigation into developing low cost alternatives. In this paper we present an inexpensive design (total cost of components: ca £30) for simulating lumbar puncture during 4cm needle displacement (Fig 2). Two versions of the device have been built and we present a comparison of their force profiles with those obtained from a lumbar puncture simulator at Ysbyty Gwynedd Hospital. This evaluation was carried out by programming our force profile, based on porcine lumbar puncture [3], into the device (Fig. 1). Force feedback from our devices and the simulator at Ysbyty Gwynedd Hospital was obtained using a force sensitive resistor.

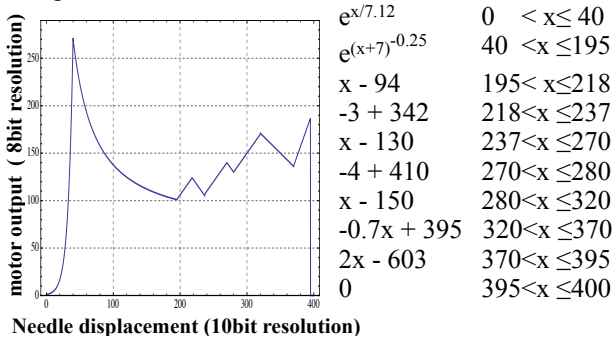


**Fig. 1** Our piecewise function, based on force feedback published by Brett *et al*. Needle displacement (x) is measured with 10 bit resolution (0 - 1023).

## MATERIALS AND METHODS

A motorised linear potentiometer (Bourns, PSM Series, 10KOhm, linear taper) with FF-050SB, Mabuchi Motor (8V, 0.023A, 6.4g.cm) was used for moving the needle and measuring its displacement (Fig. 2). The piecewise algorithm (Fig. 1) was programmed into an Arduino Mega 2560 R3 which read the potentiometer analog values during needle displacement and regulated the actuator accordingly with an Adafruit L293D motor shield. A modified version (device II) was built by removing the motor from another Bourns 10KOhm motorised potentiometer, and attaching a standard 5v motor (DC, 8V nominal, 0.04A, 120g.cm). The new motor required re-positioning on the opposite side of the drive with a 3D printed holder, from a MakerBot

Replicator 2X (Fig. 2). Joining the drive belt to the motor required a 10mm plastic cogwheel eroded with sand paper to reduce its diameter to 8mm. Force feedback was measured with a 4mm diameter force sensitive resistor (FSR - Interlink Electronics FSR™ 400) and an algorithm published by Adafruit Industries [4]. Once the sensor algorithm was calibrated with 200g, 500g, 1kg and 2kg standard masses, force data was collected for further analysis. Force feedback collected from a EIT100 Lumbar Epidural Trainer [5], at Ysbyty Gwynedd Hospital, was used for comparison with our devices.

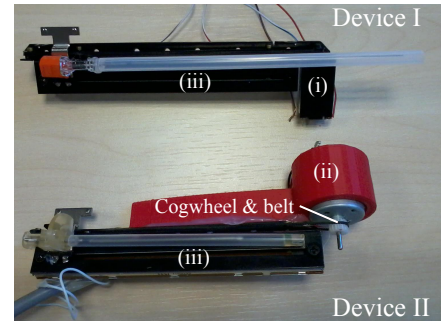


**Fig. 2** (i) FF-050SB motor (ii) 3D printed motor holder with FF-050SB motor (iii) Bourns potentiometers.

## RESULTS

	Device I / N	Device II / N
0V	1.73	6.90
	} Δ8.57	
5V	10.3	14.9
	} Δ8.00	
	Device I SD	Device II SD
0V	0.681	2.64
	} Δ2.02	
5V	2.70	4.50
	} Δ1.86	

**Table 1.** Mean force feedback in newtons (N) at 0V and 5V, with their standard deviations (SD)

## DISCUSSION

The FSR sensors require symmetrical force distribution for consistent readings and are not used to obtain precise measurements [4]. Calibration showed variation of ±0.1N at 5N and ±0.5N at 10N. Since our algorithm produced less than 10N, this variation was thought acceptable for our purposes. Device II provides greater force at 0V (Table 1) attributed to greater tensile forces and friction in its drive belt after reconfiguration with

the new motor. Its larger standard deviation (SD) at 0V is caused by vibrations sent down the drive belt from; (i) slight cogwheel non-symmetry after sanding and misalignment of its teeth with those of the belt, and (ii) motor inductance. Data shows the contribution of (i) to be greater than (ii) at 0V, but the effect of inductance is greater at 5V, seen by the similar SD increase for both devices which also interferes with the measurement of the force profile at higher voltage. The smaller  $\Delta N$  for device II at 5V is explained by its larger inherent resistance which makes it difficult to measure the force feedback contribution of its motor.

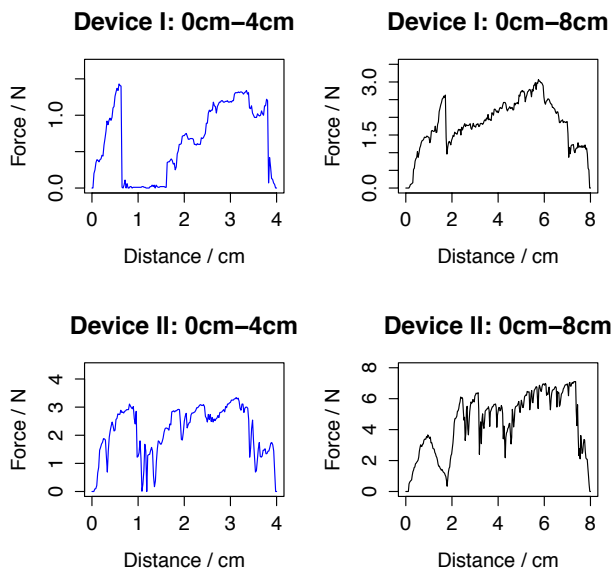


**Fig. 3** Measured force profiles for devices I and II over 0cm-4cm and 0cm-8cm.

Measured profiles (Fig. 3) do not closely follow the algorithm because they are transformed by interference forces discussed earlier, including unaccounted motor behaviour in our algorithm. For example, a quadratic best fit curve for force feedback was obtained with the following algorithms, whose domain map 8bits over the interval 0-255:  $f(x)=0$ , i.e. 00000000 or 0V,  $f(x)=16$ ,  $f(x)=32$ ,  $f(x)=64$ ,  $f(x)=128$  and  $f(x)=255$ , i.e. 11111111 or 5V (refer to y-axis of fig. 1). Derivatives are approximately: device I (0.8x-1.59) and II (1.22x-2.01), suggesting the motors provide different and non-linear force feedback at various voltages. Furthermore, doubling the displacement increases force feedback associated with the algorithm linear functions in fig. 1, and with more interference. Though device II creates greater force feedback, its profile does not show the programmed forces as clearly as device I, probably due to interference by factors (i) and (ii) above. Comparing the profiles of device I (0cm-4cm) and the EIT100 simulator (fig. 4) are similar and show the distinctive peaks, though non-linear motor behaviour and force transformations have affected the profile.

An effective haptic device should simulate the programmed force profile and magnitudes closely and consistently. Though device I better replicates the profile over 0cm-4cm displacement, the magnitudes are significantly smaller than is realistic for lumbar

puncture; device II falls short in both assessments. Transformations of the programmed force profile during use of the devices makes their current design non optimal. However, we suggest that improving the force algorithm to account for inherent force transformations in device I, could provide a more predictable output and improve its suitability for procedures that involve displacement from 0cm-4cm and forces smaller than two newtons.

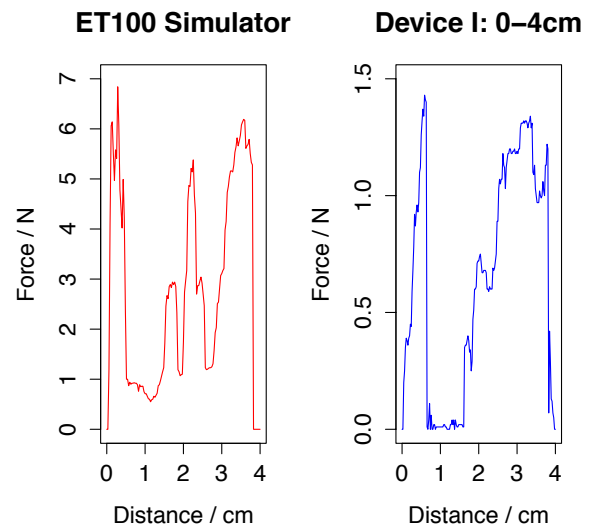


**Fig. 4** Force profile for device I (0cm-4cm) compared with an example from the EIT100 simulator.

## ACKNOWLEDGMENTS

This work was funded by the Wales National Institute for Social Care and Health Research (NISCHR) as part of the Advanced Medical Imaging and Visualisation Unit. Authors also thank Dr Iestyn, Pierce, Head of School of Electronic Engineering, Bangor University, for suggestions.

## REFERENCES

- [1] Luboz V., Hughes C., Gould D., John N. and Bello F., 2009, "Real-time Seldinger Technique Simulation in Complex Vascular Models International Journal of Computer Assisted Radiology and Surgery", vol.4/6, p 589.
- [2] Chan T., Luboz V., Hughes C., John N., Bello F., Gould D. A. "A haptically enhanced interventional radiology vascular simulator for training the Seldinger technique", Proceedings of Cardiovascular and Interventional Radiological Society of Europe (CIRSE), Lisbon, September 2009.
- [3] Brett, P. N., Harrison, a J., & Thomas, T. a. (2000). Schemes for the identification of tissue types and boundaries at the tool point for surgical needles. IEEE transactions on information technology in biomedicine: a publication of the IEEE Engineering in Medicine and Biology Society, 4(1), 30-6
- [4] Adafruit Industries. <http://learn.adafruit.com/force-sensitive-resistor-fsr/using-an-fsr>. Accessed 13th February 2014
- [5] Pharmabotics Ltd, <http://www.pharmabotics.com/lumbar-epidural-injection-and-lumbar-puncture-trainer/>. Accessed 17th February 2014